Human Molecular Genetics, 2009, Vol. 18, No. 4 **607–620**
doi:10.1093/hmg/ddn386
Advance Access published on November 13, 2008

Disruption of nesprin-1 produces an Emery Dreifuss muscular dystrophy-like phenotype in mice

Megan J. Puckelwartz[1], Eric Kessler[2], Yuan Zhang[1], Didier Hodzic[3], K. Natalie Randles[4], Glenn Morris[4], Judy U. Earley[2], Michele Hadhazy[2], James M. Holaska[2], Stephanie K. Mewborn[2], Peter Pytel[5] and Elizabeth M. McNally[1,2,*]

[1]Department of Human Genetics, [2]Department of Medicine, Section of Cardiology, [3]Department of Cell Biology, Washington University, St Louis, MO, USA, [4]Centre for Inherited Neuromuscular Disease, RJAH Orthopaedic Hospital, Oswestry SY10 7AG, UK and [5]Department of Pathology, The University of Chicago, Chicago, IL, USA

Mutations in the gene encoding the inner nuclear membrane proteins lamins A and C produce cardiac and skeletal muscle dysfunction referred to as Emery Dreifuss muscular dystrophy. Lamins A and C participate in the LINC complex that, along with the nesprin and SUN proteins, LInk the Nucleoskeleton with the Cytoskeleton. Nesprins 1 and 2 are giant spectrin-repeat containing proteins that have large and small forms. The nesprins contain a transmembrane anchor that tethers to the nuclear membrane followed by a short domain that resides within the lumen between the inner and outer nuclear membrane. Nesprin's luminal domain binds directly to SUN proteins. We generated mice where the C-terminus of nesprin-1 was deleted. This strategy produced a protein lacking the transmembrane and luminal domains that together are referred to as the KASH domain. Mice homozygous for this mutation exhibit lethality with approximately half dying at or near birth from respiratory failure. Surviving mice display hindlimb weakness and an abnormal gait. With increasing age, kyphoscoliosis, muscle pathology and cardiac conduction defects develop. The protein components of the LINC complex, including mutant nesprin-1α, lamin A/C and SUN2, are localized at the nuclear membrane in this model. However, the LINC components do not normally associate since coimmunoprecipitation experiments with SUN2 and nesprin reveal that mutant nesprin-1 protein no longer interacts with SUN2. These findings demonstrate the role of the LINC complex, and nesprin-1, in neuromuscular and cardiac disease.

INTRODUCTION

The nuclear envelope divides the functions of the cytoplasm from those of the nucleus. The nuclear envelope is composed of the outer nuclear membrane, the inner nuclear membrane and the intervening perinuclear space. The inner nuclear membrane faces the nucleoplasm and is supported by the lamina, composed of the A- and B-type lamins. The lamins are type V intermediate filament proteins that associate with the nuclear membrane through integral membrane proteins. B-type lamins are expressed in all somatic cells, while the A-type lamins, lamins A and C, are alternatively spliced isoforms transcribed from the *LMNA* gene and are expressed in all terminally differentiated tissues. The lamina is a fibrous structure that provides shape and support to the nucleus. The lamina also plays an epigenetic role in gene expression as it acts as a scaffold for chromatin (1).

Mutations in the *LMNA* gene cause Emery Dreifuss muscular dystrophy (EDMD), a disorder of progressive skeletal muscle weakness associated with muscle contractures and heart disease that preferentially targets the conduction system of the heart. The gene encoding the nuclear membrane protein, emerin, is also associated with a similar constellation of defects except that the mode of inheritance differs with X-linked recessive inheritance. *LMNA* mutations causing heart and skeletal muscle disease exhibit marked inter- and intra- familial variability in disease phenotype indicating the involvement of genetic modifiers in the progression of the disease (2). Several murine models of *LMNA* gene mutations also recapitulate the EDMD phenotype (3–5) demonstrating

*To whom correspondence should be addressed at: The University of Chicago, 5841 S. Maryland, MC6088, Chicago, IL 60637, USA. Tel: +1 773 702 2672; Fax: +1 773 702 2681; Email: emcnally@uchicago.edu

© *The Author 2008. Published by Oxford University Press. All rights reserved.*
For Permissions, please email: journals.permissions@oxfordjournals.org

the importance of the nuclear membrane in neuromuscular disease. Interestingly, most *LMNA* mutations are autosomal dominant and most components of the nuclear membrane remain tethered to the nuclear membrane. In both human and murine models, it is assumed that the nuclear lamina, while normally positioned, is abnormally assembled leading to mechanical and functional deficits (1,5–11). Approximately 60% of patients with EDMD or EDMD-like phenotypes do not have mutations in either *LMNA* or emerin indicating that mutations in other genes also cause EDMD-like phenotypes (12).

Recently, missense changes were described in the genes encoding the nuclear envelope proteins nesprin-1 and -2. These findings were in relatively small families with only one or two affected members where there was a range of phenotypes that included elevated creatine kinase to those with more EDMD-like features (13). Two missense changes were described in nesprin-1, in the region shared in the nesprin-1α isoform. The isolated nesprin-1 missense changes were described in single individuals, and thus family history was unavailable to confirm segregation of the genotype with the phenotype. One missense change in nesprin-2 was reported and thought to affect the nuclear envelope isoform, nesprin-2β (13). Nesprins (also known as syne, myne, nuance, enaptin) 1 and 2 are members of a spectrin repeat family of proteins (14–17). In their full-length form, the nesprin genes encode proteins up to 1 MDa in size with an actin-binding site at the N-terminus and spectrin repeats along the length. The C-terminus contains the KASH domain (Klarsicht, ANC-1 and Syne homology), a conserved protein motif of approximately 60 amino acids that includes a transmembrane domain followed by a luminal domain of approximately 40 amino acids residing in the perinuclear space. Alternative promoter usage and splicing produces shorter forms containing spectrin repeats and the KASH domain (14,18). The larger nesprin forms are thought to reside in the outer nuclear membrane while the shorter forms are tethered to the inner nuclear membrane. One short form, referred to as nesprin-1α, is highly expressed in cardiac and skeletal muscle (14,15). Cell-based expression studies have shown that the localization of the nesprins in the nuclear envelope is dependent on SUN domain-containing proteins and requires the KASH domain of nesprin (14,19,20). SUN proteins in turn bind with lamin A/C in the nucleus creating a bridge linking the nucleus to the cytoplasm termed the LINC complex (21).

In order to explore the role of nesprin-1 in the pathology of muscle disease, we generated mice lacking the KASH domain and refer to these as Δ/ΔKASH mice. Δ/ΔKASH mice lack the entire C-terminal KASH domain and instead have an alternate protein sequence that is not homologous to any known protein domain. Δ/ΔKASH mice exhibit ∼50% perinatal lethality. Surviving mice have a progressive muscle wasting disorder that is associated with an abnormal gait and kyphoscoliosis. In addition, cardiac defects are present. In human patients with heterozygous *LMNA* mutations, lamin A/C and emerin, components of the LINC complex, are normally localized in cardiac and skeletal muscle (6–8,10). In the model we present here, the LINC complex proteins are also normally localized, but the resulting phenotype is consistent with abnormal function. Therefore, the Δ/ΔKASH mice serve as a model for nesprin-1's role in neuromuscular disease and EDMD.

RESULTS

Generation of Δ/ΔKASH mice

We used homologous recombination to delete the 3′ most terminal coding exon of nesprin-1 because this exon encodes the transmembrane domain and short luminal segment that contribute to the KASH domain. LoxP sites were inserted on either side of the terminal exon in a position 200 bp 5′ of the first codon and 200 bp downstream of the 3′-UTR (Fig. 1A). Southern blotting was used to confirm homologous recombination (Fig. 1B). Mice with a floxed terminal exon were bred to mice expressing cre in the male germline (22). PCR confirmed recombination of loxP sites resulting in deletion of the neo cassette and the terminal exon (Fig. 1C). We amplified the mRNA produced from the Δ/ΔKASH allele and used 3′ RACE to determine that the mutant mRNA lacks the two terminal exons and contains an additional 183 bp (Fig. 2A). The sequence of the ΔKASH allele predicts a protein that lacks the 100 C-terminal amino acids with replacement of these amino acids by an alternate 61 amino acids. Database searches revealed no homology between these 61 amino acids and known protein domains (Fig. 2C). Immunoblotting was performed with an anti-nesprin-1 antibody that recognizes an epitope within both the wild-type and ΔKASH nesprin-1 protein. Nesprin-1α, the 120 KDa splice form highly expressed in striated muscle, was readily detectable in wild-type and Δ/ΔKASH skeletal muscle and differentiated primary myoblasts. The size of the ΔKASH protein was close to the size of wild-type protein given the deletion of 100 amino acids and the insertion of 61 amino acids (Fig. 2B). This result was confirmed with an alternative and independently generated anti-nesprin-1 antibody MANNES1A (data not shown). In Δ/ΔKASH muscle, nesprin-1α is expressed at normal levels but contains an alternate C-terminus (Fig. 2C).

Loss of the KASH domain causes perinatal lethality

Genotyping of 333 offspring from intercrosses of heterozygous +/ΔKASH mice demonstrated that half the expected number of mutant mice was seen at 21 days of age (Fig. 3A). There was no difference in survival between males and females. To determine when Δ/ΔKASH mice die, we genotyped embryos from heterozygous intercrosses between embryonic day 17.5 and birth (P0). The expected 25% ratio of Δ/ΔKASH mice was present at E17.5–P0 suggesting that Δ/ΔKASH mice die between P0 and 21 days of life (Fig. 3A). We also found no difference in the sex ratio (50% male and female, $n = 8$ each) in the E17.5–P0 compared with the P21 mice indicating that males and females die in equal ratios. P1 mice were genotyped, and we found that only 13% of the mice were mutant. This is approximately half the expected 25% Mendelian ratio ($P < 0.05$). Taken together with the data from the late embryonic stages, we conclude that Δ/ΔKASH mice have perinatal lethality, dying just prior to, at or near birth. To determine if Δ/ΔKASH mice were alive at birth, live births from heterozygous intercrosses were monitored. Δ/ΔKASH pups were smaller than wild-type littermates and sometimes appeared cyanotic. These mice only survived ∼10–15 min after birth;

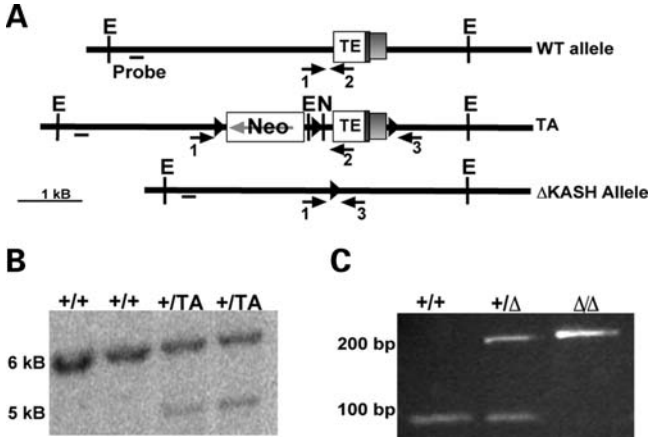

Figure 1. Gene targeting of nesprin-1 KASH domain. (**A**) The targeting allele (TA) included the KASH domain-containing terminal exon (TE, KASH domain=dark gray box, 3′-UTR=light gray box) surrounded by loxP sites and an upstream neomycin cassette. Cre-recombinase was used to remove the neomycin cassette and TE. (**B**) Southern blot demonstrating homologous recombination of the targeted allele. *Eco*RI digested embryonic stem cell DNA was blotted and hybridized with the probe shown in (A). (**C**) PCR genotyping of tail DNA was performed with primers 1, 2 and 3, indicated as arrows in (A), to confirm deletion of the terminal exon. Primer 1, located upstream of the terminal exon and primer 2, located within the terminal exon, yield a 90 bp band in wild-type mice. Primer 3 is located outside of the terminal exon and in conjunction with primer 1 will produce a 254 bp product in Δ/ΔKASH mice.

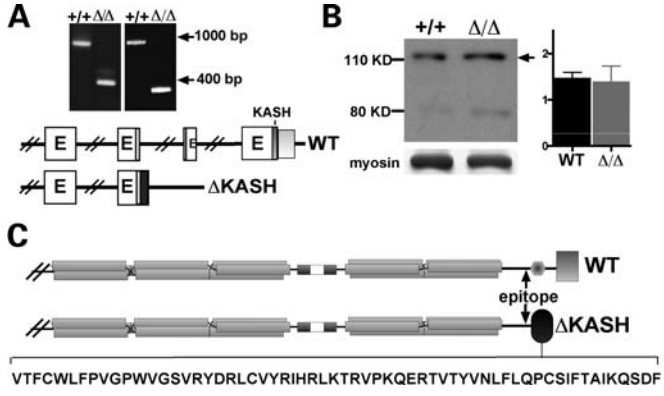

Figure 2. Deletion of the nesprin-1 KASH domain leads to translation of a truncated protein, ΔKASH. (**A**) 3′RACE was performed on both wild-type and Δ/ΔKASH cDNA. Wild-type cDNA produced the expected 972 bp band, Δ/ΔKASH cDNA produces a 359 bp band corresponding to loss of the last two exons and addition of 183 bp. The image on the left represents the first round of 3′RACE and the gel on the right is the second round from the nested reaction. Below that is a schematic of the genomic region indicating transcribed exons in WT and Δ/ΔKASH mice. In WT mice, the terminal exon contains the KASH domain (dark gray) and the 3′-UTR (light gray). The antibody epitope is indicated by the stippling. In Δ/ΔKASH mice the terminal exon is deleted and readthrough occurs resulting in an mRNA lacking the two terminal exons and containing an additional 183 bp (black). (**B**) Immunoblotting from skeletal muscle isolated from wild-type (+/+) littermate and Δ/ΔKASH mice express a nesprin-1α isoform that migrates at 120 kDa, indicated by the arrow. The myosin band is shown as a loading control. Densitometry was performed comparing both wild-type and Δ/ΔKASH immunoblotting bands to loading controls. The ratio between signal and control for six wild-type and seven Δ/ΔKASH bands were compared and are shown in the graph provided. There is no significant difference between wild-type and Δ/ΔKASH protein levels. (**C**) Protein schematic of normal nesprin-1α and ΔKASH. Nesprin-1α normally contains five spectrin repeats (gray bars) and a C-terminal KASH domain (gray box). The ΔKASH protein is also predicted to contain five spectrin repeats but is missing 100 amino acids encoded by the last two exons and instead has 61 amino acids at its C-terminus. These additional 61 residues have no predicted relationship to any known protein (black oval) and do not encode a transmembrane domain. The novel amino acids encoded by the ΔKASH allele are shown at the bottom.

wild-type pups were $1.7 \pm .03$ g and surviving mutant Δ/Δ pups were $1.4 \pm .02$ g ($P < 0.0001$, $n = 8$ and 14, respectively) (Fig. 3B). Mice were sacrificed after birth and their lungs were examined. Wild-type lungs were expanded and buoyant in water, while lungs from cyanotic pups were small and lacked buoyancy indicating that the lungs of these Δ/ΔKASH mice did not inflate (Fig. 3C). Forty-nine percent of Δ/ΔKASH mice die by P21 consistent with half surviving beyond the perinatal period (Fig. 3A).

Female Δ/ΔKASH mice are small and uncoordinated

Surviving Δ/ΔKASH mice were studied further. Whole body mass of Δ/ΔKASH mice and their wild-type littermates was recorded each week from 3 to 20 weeks of age. Female Δ/ΔKASH mice were significantly smaller ($P < 0.0001$) than wild-type littermate female mice throughout the 20 weeks ($n = 7$ wild-type, $n = 8$ Δ/ΔKASH) (Fig. 4A). While some male Δ/ΔKASH mice appeared smaller than wild-type littermates, this was an inconsistent phenotype and was not significantly different between the two groups in this age group ($n = 7$ each genotype, data not shown). To determine if the Δ/ΔKASH mice had a muscle defect, mice were run on a rotarod. As illustrated in Figure 4C, wild-type mice maintained an upright posture on the rod. In contrast, Δ/ΔKASH mice remained on the rod but with an abnormal posture where their bodies were perpendicular to the top of the rod. We measured the degree to which mice were displaced on the rotarod where an angle of 0 was scored when the shoulders were parallel to the bar and increasing angles were scored as the shoulders rotated back. The same group of mice ($n = 3$ female, 3 male each genotype) was tested each week for 16 weeks. The average angle over multiple runs was calculated for each mouse. Female Δ/ΔKASH mice could not maintain an upright stance on the rotarod exhibiting a more downward rotation than their wild-type female littermates ($P < 0.003$) (Fig. 4B). There were no differences between the male mice (data not shown). Of note, female Δ/ΔKASH mice did not fall from the rotarod, as can be seen with uncoordinated phenotypes. In contrast, female Δ/ΔKASH mice maintained a tight grip with their forelimbs and thus displayed a preferential weakness of their hindlimbs.

Δ/ΔKASH mice display kyphoscoliosis

A common defect in human patients with muscular dystrophy is kyphosis and scoliosis that arises from paraspinal muscle weakness as well as contractures of the spine. We examined both male and female Δ/ΔKASH mice between 9 and 12 months old and found that older Δ/ΔKASH mice developed severe kyphoscoliosis (Fig. 5A). Older Δ/ΔKASH mice also exhibit poor grooming as was evidenced by a scruffy coat and ocular conjunctivitis (Fig. 5B). Older mice had difficulty grooming due to weakness and stiffness that appeared to

A Survival of progeny from heterozygous intercrosses

Nesprin-1 genotype frequency					
	+/+	+/Δ	Δ/Δ	total	p
E17.5-P0	15 (14.5)	24 (29)	19 (14.5)	58	>0.05
P1	18(15)	34 (30)	8 (15)	60	<0.05
P21	87 (83.25)	205 (166.5)	41 (83.25)	333	<0.001

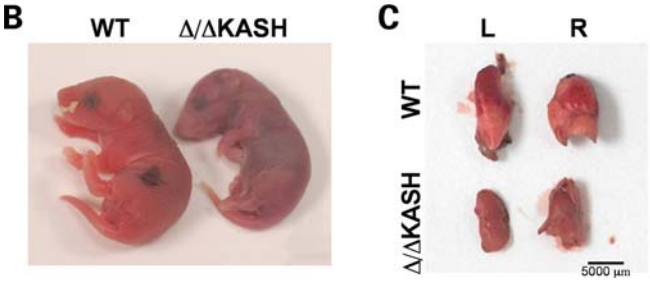

Figure 3. Respiratory failure in Δ/ΔKASH neonatal mice. (**A**) Survival of progeny from heterozygous intercrossed mice. Mice were genotyped between embryonic days 17.5 (E17.5) and birth (P0), at post-natal day 1 (P1) and at 21 days of life (P21). The number of mice observed is indicated for each genotype and the expected is shown in parentheses. Less than half the expected number (49%) of Δ/ΔKASH mice were seen at P21, but they were present at late stage development indicating perinatal lethality. (**B**) The Δ/ΔKASH mouse appears smaller and cyanotic. (**C**) Lungs were removed from WT and Δ/ΔKASH P0 mice immediately after sacrifice. The Δ/ΔKASH lungs are not expanded consistent with respiratory failure at birth. L and R indicate left and right lungs, respectively.

limit the range of motion of their limbs. Kyphoscoliosis, eye infections and poor grooming were noted beginning at 7 months of age in both male and female Δ/ΔKASH mice. We weighed mice between 8 and 12 months of age and found that female Δ/ΔKASH mice continue to weigh significantly less than their wild-type littermates (wild-type 25.2 ± 1.5 g, Δ/ΔKASH$=18.3 \pm 0.93$ g, $n = 6$ and 8, respectively, $P = 0.0014$). At this advancing age, we also found that mutant male mice weighed significantly less than their wild-type littermates (wild-type$=31.7 \pm 2.3$ g and Δ/ΔKASH 23.3 ± 2.6 g, $n = 5$ and 6, respectively, $P = 0.04$). We also noted that by 16 months of age, all Δ/ΔKASH mice, both male and female, displayed some kyphoscoliosis and scruffy coat. In order to better illustrate this point, Figure 5A and B are male 9–11-month-old mice. These data indicate that male Δ/ΔKASH mice have a similar phenotype that has later onset than female mice.

Δ/ΔKASH hindlimb muscle has pathological defects

Rotarod data suggested that the Δ/ΔKASH mice had hindlimb muscle weakness. We examined soleus muscle for defects in nuclear localization and fiber size (Fig. 6A). Using muscle from both male and female 9–13-month-old Δ/ΔKASH mice ($n = 4$, two male and two female) and their wild-type littermates ($n = 3$, one female and two male), we found that the Δ/ΔKASH mice have significantly more centrally placed nuclei than wild-type ($P = 0.0023$) (Fig. 6B). We next measured fiber size between Δ/ΔKASH and wild-type and

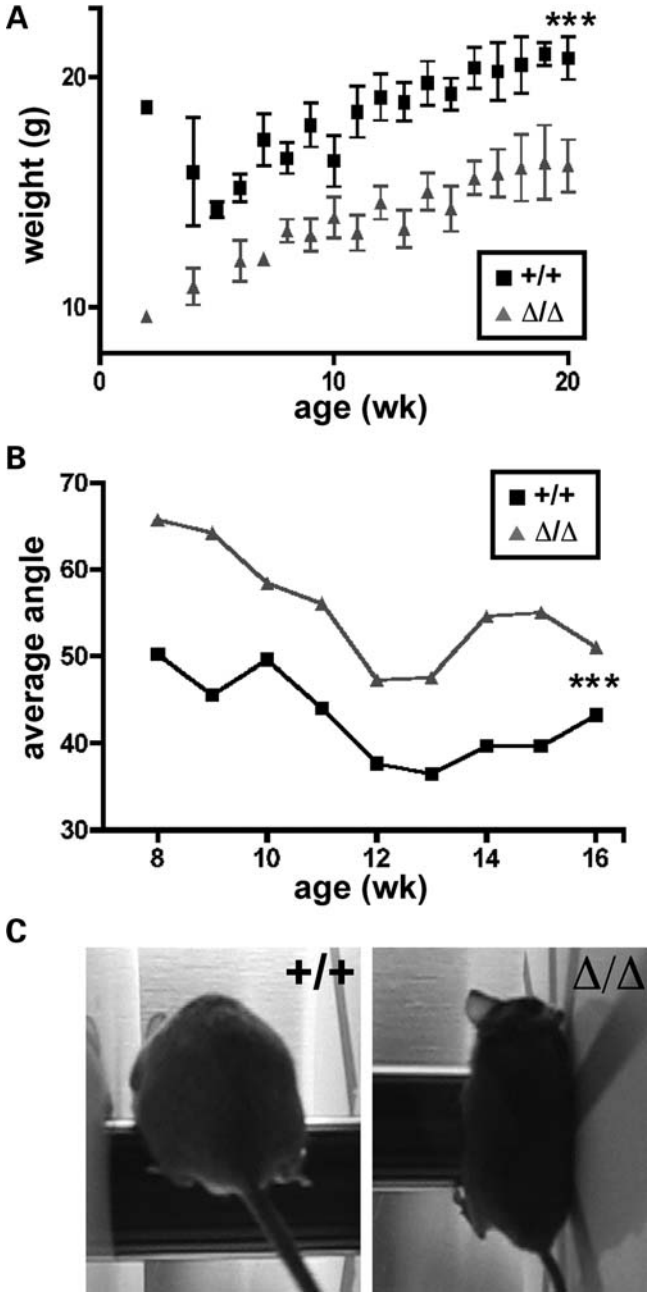

Figure 4. Female Δ/ΔKASH mice are small and uncoordinated. (**A**) Whole body mass of WT (+/+) littermates (black squares) and Δ/ΔKASH (gray triangles) female mice differ significantly $P < 0.0001$, where Δ/ΔKASH mice are much smaller ($n = 7$ wild-type, $n = 8$ Δ/ΔKASH). (**B**) Female Δ/ΔKASH mice do not maintain horizontal position on the rotarod bar as indicated by increased average running angle when compared with age matched controls, ($n = 3$ female mice per genotype, age 8–16 weeks), $P < 0.0003$, as illustrated in (**C**).

found that the Δ/ΔKASH mice have significantly smaller fibers in the soleus muscle of the hindlimb ($P < 0.0001$) (Fig. 6B). Δ/ΔKASH mice also have larger variation in fiber size than their wild-type littermates in the soleus muscle as the mean fiber size for wild-type is 1646 ± 25.22 and 1158 ± 53.55 μm^2 for Δ/ΔKASH mice. The distribution of fiber size revealed an overrepresentation of smaller fibers in

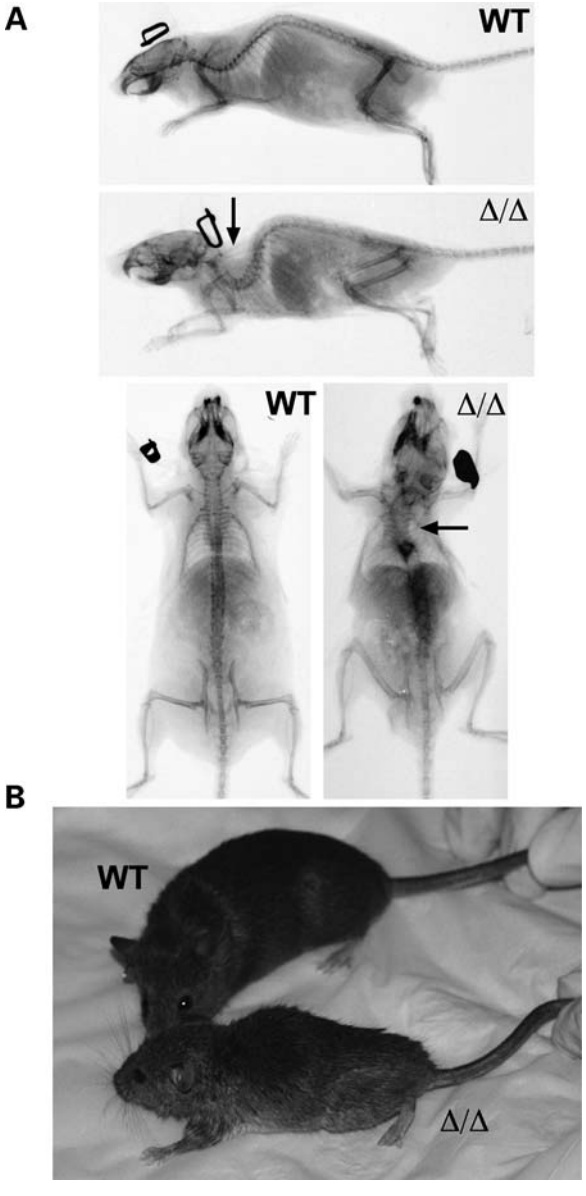

Figure 5. Δ/ΔKASH mice exhibit kyphoscoliosis. (**A**) Lateral and posterior–anterior view X-rays of 9–11-month-old WT littermate and Δ/ΔKASH male mice. The Δ/ΔKASH mouse exhibits severe kyphoscoliosis as indicated by arrows. (**B**) Photographs of mice from (A), note the small size and scruffy coat of the Δ/ΔKASH mouse indicating poor grooming capabilities.

the Δ/ΔKASH mice compared with wild-type littermates (Fig. 6C). Similar trends were seen for the gastrocnemius muscle (data not shown). The combination of fiber size variation and increased central nucleation is consistent with what is seen in patients with EDMD.

Nuclei localize abnormally in Δ/ΔKASH muscle fibers

The Syne-1 and -2 null mouse models have disorganized nuclei (23). To determine if the Δ/ΔKASH mice have nuclear positioning defects, we teased fibers from both triceps and tibialis anterior of 8–12-week-old ($n = 2$ wild-type, $n = 3$ Δ/ΔKASH) and 9–12-month-old ($n = 2$ wild-type, $n = 2$ Δ/ΔKASH) male and female mice. The fibers were stained with DAPI and whole mounted. The nuclei in Δ/ΔKASH mice were disorganized compared with wild-type littermates. In both young and old wild-type mice nuclei were aligned in a row along the length of the fiber, while in young and old Δ/ΔKASH mice, nuclei were clustered and non-aligned (Fig. 6D). Zhang *et al*. (23) also demonstrated that synaptic nuclei were no longer anchored to the neuromuscular junction in their Syne-1 null mouse model. We have also examined the nuclei under the neuromuscular junction in Δ/ΔKASH mice and find that they are no longer associated with the junction (data not shown). While our data is consistent with earlier work that disruption of nesprin causes mislocalization of both non-synaptic and synaptic nuclei, the Syne-$1^{-/-}$ mouse model does not exhibit a clinical muscle phenotype (23), while the Δ/ΔKASH mice have muscle disease. The discordance in phenotypes between these models argues that nuclear mislocalization is not responsible for the muscle defect.

Δ/ΔKASH mice exhibit cardiac conduction system defects

Cardiac conduction system abnormalities are a hallmark of EDMD in humans. Therefore, we used ambulatory electrocardiography (ECG) on 9–12-month-old males and females to determine whether Δ/ΔKASH mice displayed conduction system defects ($n = 2$ wild-type, male; $n = 3$ Δ/ΔKASH, 1 female, 2 male). Both male and female mice were used because at this advanced age we noted that both sexes have reduced mass compared with wild-type littermates and both display kyphoscoliosis and poor grooming indicating muscle disease. Representative ECG tracings are shown in Figure 7A. Δ/ΔKASH mice have a prolonged PR interval ($P < 0.0001$) indicative of conduction system block at the level of the atrioventricular node. Mutant mice also have a widened QRS ($P < 0.0001$) consistent with disease affecting the ventricular conduction system (Fig. 7B).

Nesprin-1 and Lamin A/C localize normally in Δ/ΔKASH mice

In order to determine whether ΔKASH protein could localize to the nuclear membrane we performed immunostaining on muscle sections from 8- to 12-week-old (Fig. 8) and 9- to 12-month-old (data not shown) male and female mice using an anti-nesprin-1 antibody that recognizes both wild-type nesprin-1α and ΔKASH protein. Nesprin-1α localized to the nuclear envelope in both wild-type and Δ/ΔKASH mice suggesting that the KASH domain is dispensable for the normal localization of nesprin-1α to the nuclear membrane. The additional amino acids added to the C-terminus of nesprin-1 do not contain a hydrophobic stretch and harbor no sequence that is predicted to function as a transmembrane domain. Prior over-expression studies in various cell types indicated that the transmembrane domain of nesprin-1α was important for nuclear localization (14,24). We overexpressed the Δ/ΔKASH protein in differentiated C2C12 cells and determined that it properly localizes to the nuclear membrane indicating that the KASH domain is not required for localization (data not shown). However, despite the absence of a

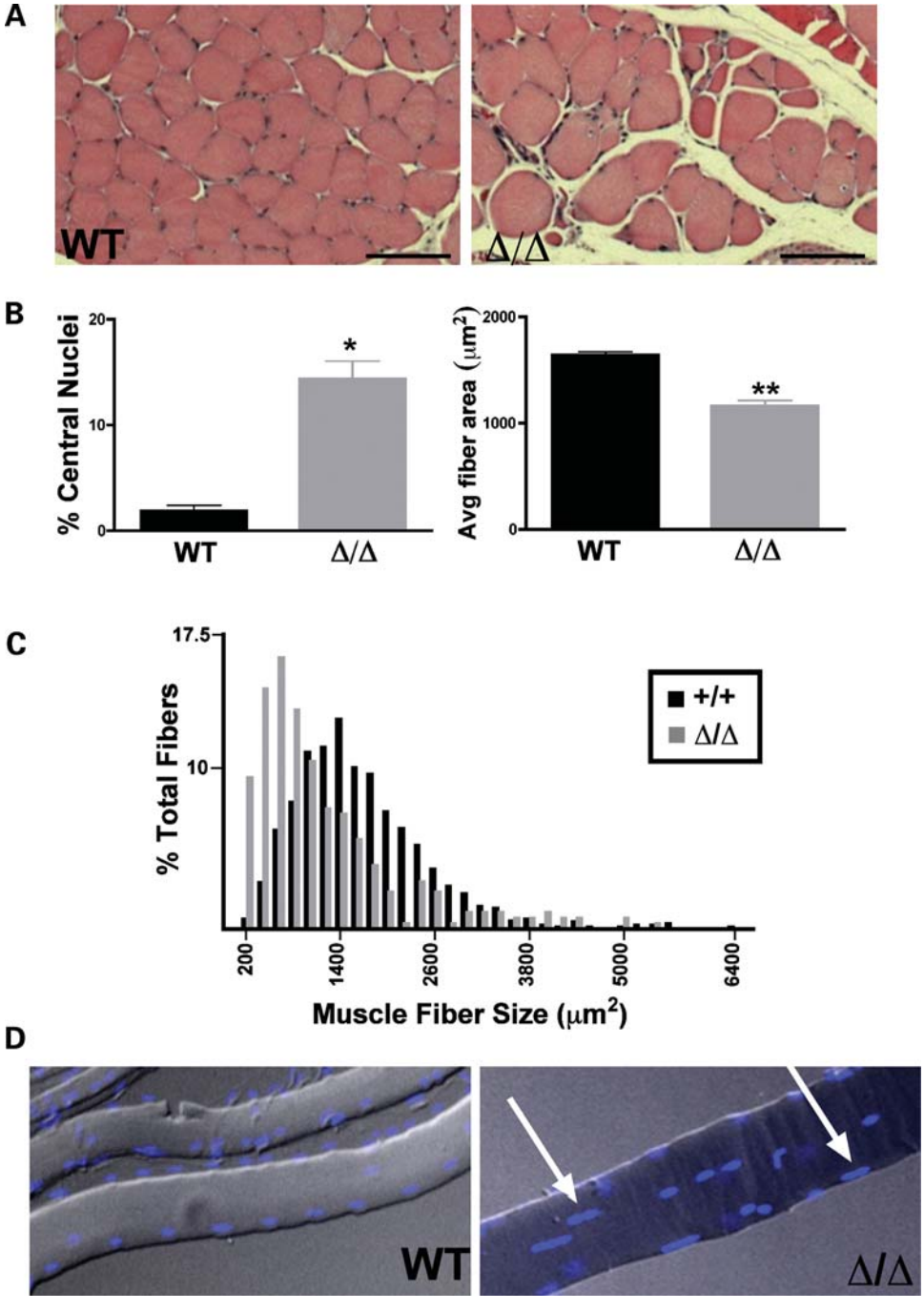

Figure 6. Δ/ΔKASH mice have muscle pathology. (**A**) Cross-section of soleus muscle from 9- to 13-month-old wild-type and Δ/ΔKASH mice. The scale bar represents 100 μm. (**B**) Graphs indicating that Δ/ΔKASH mice have greater numbers of central nuclei and decreased fiber size in soleus muscle compared with wild-type ($n = 4$, two male, two female Δ/ΔKASH; $n = 3$, two male, one female wild-type). (**C**) Histogram of muscle fiber area from wild-type and Δ/ΔKASH mice indicating that Δ/ΔKASH mice have an increase in the number of small myofibers. (**D**) Tibialis anterior muscle fibers from wild-type and Δ/ΔKASH skeletal muscle were teased apart and stained for nuclei. Wild-type myofibers have nuclei arranged in long rows, while Δ/ΔKASH myofiber nuclei are clumped (arrows).

hydrophobic transmembrane domain, it is possible that the additional 61 amino acids of the Δ/ΔKASH protein mediate localization to the nuclear membrane in some unknown manner. Alternatively, overexpression and/or expression in heterologous cells such as COS7 may not recapitulate the full complexity of the LINC complex found in mature myofibers consistent with nesprin-1α having additional binding partners at the nuclear envelope *in vivo*. To this point, nesprin-1 has been shown to interact directly with lamin A/C, both *in vitro* and *in vivo* (25,26). *In vitro*, the final two spectrin repeats of nesprin-1α were sufficient to mediate this interaction, and importantly, the interaction between nesprin-1α and lamin A

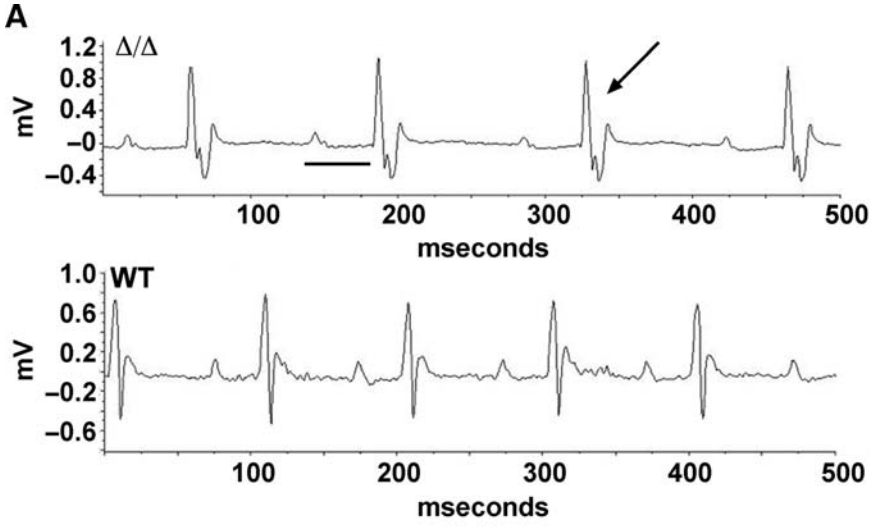

B

	+/+ n=2	Δ/Δ n=3
HR (bpm) *	601.3 ± 0.605	536 ± 0.581
QRS interval (ms)*	13.53 ± 0.00	16.28 ± 0.00
PR Interval (ms) *	41 ± 0.00	45.6 ± 0.00
QT_c Interval (ms)*	82.89 ± 0.00	87.26 ± 0.00

Figure 7. ECG analysis Δ/ΔKASH mice. (**A**) Ambulatory ECG tracing from male 9–12-month-old WT and Δ/ΔKASH mice. Δ/ΔKASH have a prolonged PR interval (black line) and a widened QRS (arrow) compared with wild-type indicating conduction system disease ($n = 2$ male wild-type, $n = 3$, one female, two male Δ/ΔKASH). (**B**) Data was compiled from 24 to 30 h of ECG tracing using Physiostat software. Δ/ΔKASH mice have an elongated PR interval and a widened QRS indicative of conduction system defects. HR (bpm), heart rate beats per minute; QTc, corrected QT interval; ms, milliseconds; * indicates $P < 0.0001$.

did not require nesprin-1's KASH domain (25). Therefore, it is possible that nesprin-1α binds to the nuclear membrane through its direct interaction with lamin A, an interaction that does not require the KASH domain.

Components of the LINC complex retain nuclear membrane localization in Δ/ΔKASH muscle

Crisp *et al*. (21) recently identified the LINC complex that links the nucleoskeleton to the cytoskeleton. The LINC complex is postulated to include KASH domain-containing nesprin proteins that bind actin, SUN proteins in the perinuclear space of the nuclear envelope and lamins in the nucleus. The SUN domain of the SUN proteins extends into the perinuclear space and interacts with the KASH domains of nesprin-1, -2 and -3 (19–21). We evaluated the localization of SUN2, emerin and LAP2β and found that these components of the LINC complex were situated normally at the nuclear membrane in the nuclei in skeletal muscle myofibers from 8- to 12-week-old male and female mice (Fig. 9). This pattern of normal LINC localization was identical in older animals (ages 9–12 months), indicating that mislocalization of these proteins is not responsible for the cardiac and skeletal muscle disease found in the older Δ/ΔKASH animals (data not shown). We also examined the expression level of nesprin-2 and found that nesprin-2 levels do not differ between Δ/ΔKASH muscle and wild-type (Fig. 9D). Shown are results for the nesprin-2β isoform.

We conducted immunoprecipitation experiments using proteins from primary myoblasts isolated from both wild-type and Δ/ΔKASH mutant muscle that were then differentiated into myotubes. In wild-type myotubes, an interaction between SUN2 and nesprin-1α was detected while in Δ/ΔKASH mutant muscle, there was no detectable interaction between the Δ/ΔKASH protein and SUN2 (Fig. 9E). We further confirmed this finding by expressing wild-type nesprin-1α and the Δ/ΔKASH protein in COS7 cells followed by immunoprecipitation. In these experiments, the Δ/ΔKASH variant was identical to that produced in the mutant mouse such that the KASH domain was deleted and the additional 61 amino acids were added. Both nesprin-1α and Δ/ΔKASH were tagged with the Xpress epitope. SUN2 was tagged with a Flag epitope. Immunoprecipitation directed at SUN2 using an anti-flag antibody successfully pulled down wild-type

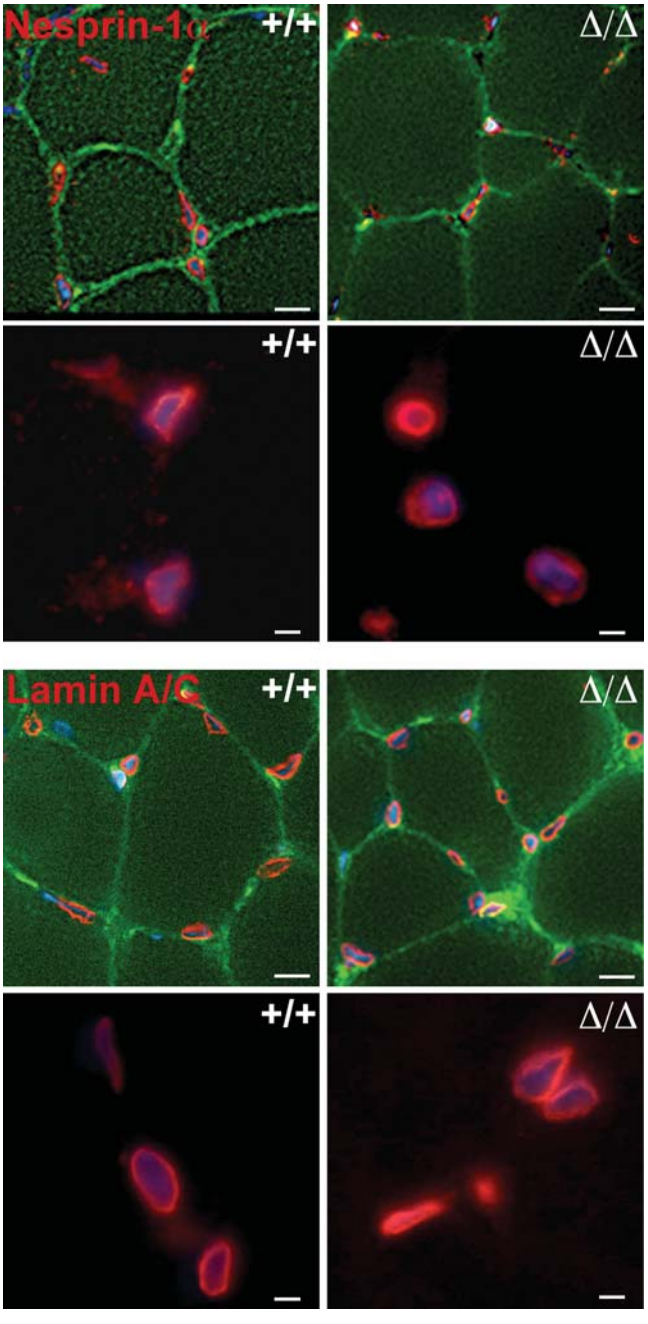

Figure 8. The KASH domain is not required for nuclear localization of nesprin-1 and lamin A/C. Top panels: Quadriceps muscle from 8- to 12-week-old littermate WT (+/+) and Δ/ΔKASH mice was sectioned and analyzed by immunofluorescence microscopy using antibodies for nesprin-1 (red) and dystrophin (top rows, green). Bottom panels: Lamin A/C also localizes normally at the nuclear membrane (shown in red, dystrophin in green). DAPI shows nuclei (blue). The top rows are shown at 40× magnification to provide muscle fiber context, while the bottom rows are 63× magnification to visualize nuclear rim staining. Scale bar 40× = 10 μm, 63× = 5 μm.

nesprin-1α but did not pull down Δ/ΔKASH demonstrating that the mutant protein has lost its interaction with SUN2 (Fig. 9F).

Therefore, the normal localization of the LINC components is not accompanied by normal interaction of the components. Specifically, the nesprin-1α - SUN interaction was disrupted, and this is modeled in Figure 10. Recent *in vitro* binding studies showed that the KASH domain of nesprin-1 directly associates with both SUN1 and 2 (27). These studies also found that adding 13 amino acids onto the C-terminus of nesprin's KASH domain is sufficient to disrupt interaction with the SUN proteins. Further mapping studies refined the interaction between SUN2 and a synthetic peptide representing the terminal 23 amino acids of KASH1. These data indicate that the C-terminus of the KASH domain is vital for the SUN2 interaction (27). Since it is this region that has been deleted in the Δ/ΔKASH mouse model, it is expected that the direct interaction between nesprin-1 and SUN is disrupted. Since the SUN proteins can also directly bind lamin A (20), some interactions within the LINC complex are likely still present in the Δ/ΔKASH mouse but these interactions do not protect against muscle disease.

DISCUSSION

Proteins of the inner nuclear membrane have been implicated in muscle disease. Recently, human patients with an Emery Dreifuss-like phenotype were described with missense changes in the genes encoding nesprin-1 and nesprin-2 (13). In order to further elucidate nesprin-1's role in muscle disease, we created a mouse lacking the terminal exon of nesprin-1. Nesprins have been shown to participate in the LINC complex that links the cytoplasm to the nucleus (21). The LINC complex is thought to include both larger and smaller forms of nesprin where the larger forms that contain an actin binding domain are confined to the outer nuclear membrane and the smaller forms that lack this domain reside on the inner nuclear membrane. Both large and small forms of nesprin rely on the transmembrane KASH domain to tether to the nuclear membrane. With this topology, the luminal portion of the KASH domain interacts with the SUN proteins to complete the link from the nuclear lamina to the actin cytoskeleton in the cytoplasm (20,23). The LINC complex is thought to have multiple contact points because the SUN proteins also interact with the lamins at the inner nuclear membrane (20), and the smaller isoforms of nesprin-1 are anchored at the inner nuclear membrane and interact with lamin A/C, both *in vitro* and *in vivo* (Fig. 10) (25,26). We now deleted the transmembrane and KASH domain portions of nesprin-1 and found that the LINC complex appears to localize normally. Namely, lamins A and C, SUN2 and nesprin-1 itself were all positioned at the nuclear membrane in both young and old animals. However, immunoprecipitation experiments indicated that ΔKASH protein could no longer interact with SUN2 leading to a dysfunctional LINC complex. Also, the phenotype arising from the loss of the KASH domain is consistent with an abnormally functioning LINC complex. In patients and model systems with lamin A/C mutations, the lamina also remains intact in cardiac and skeletal muscle even though it is functionally disrupted (1,5–11).

Interestingly, in the model we generated, deletion of the terminal exon causes an aberrant splicing event in the mutant mRNA resulting in loss of the final two exons and

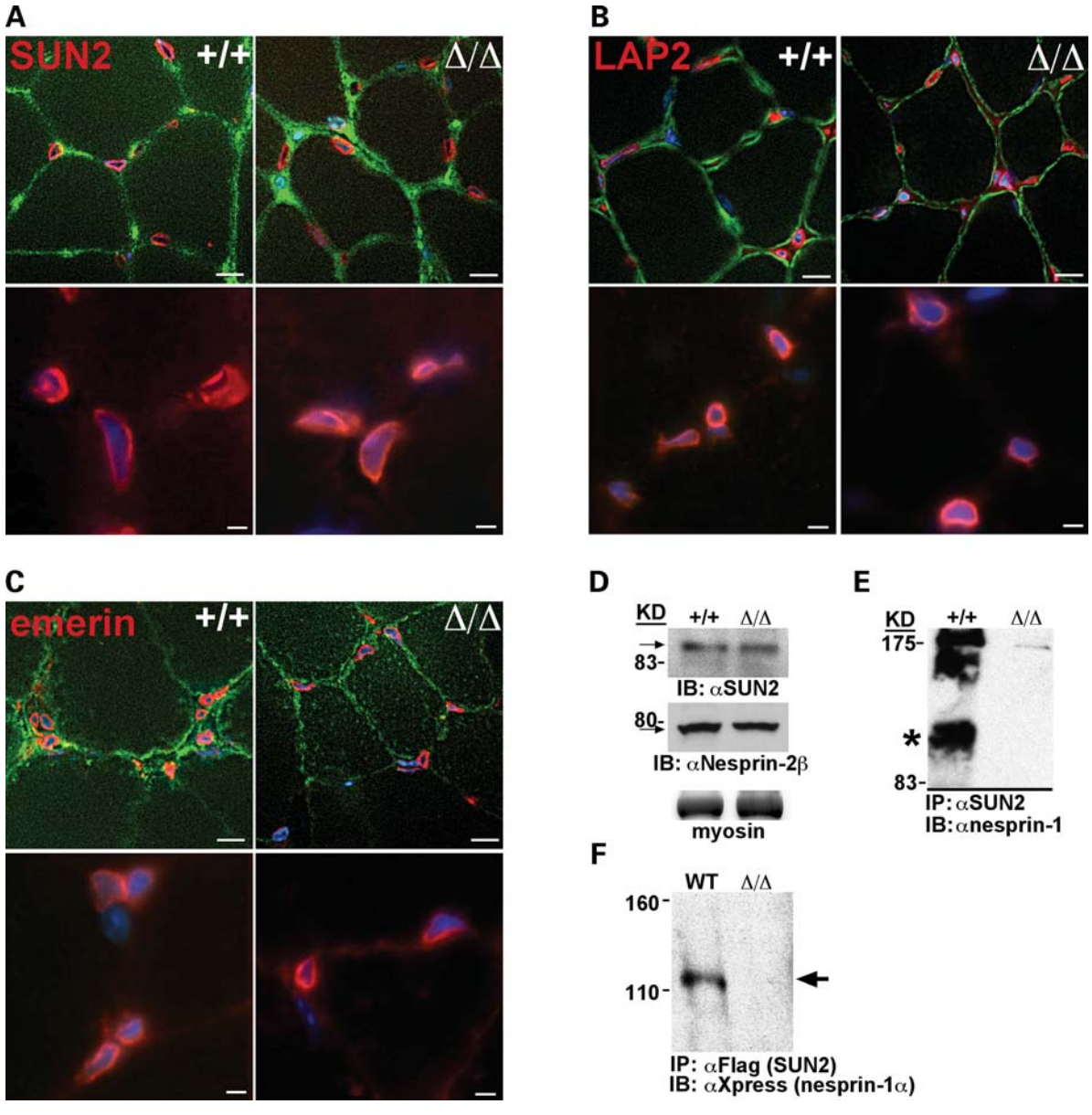

Figure 9. The LINC complex is assembled in Δ/ΔKASH mice. Quadriceps muscle from 8–12-week-old WT (+/+) littermate and Δ/ΔKASH mice was sectioned and analyzed by immunofluorescence microscopy for the localization of the LINC complex proteins, (**A**) SUN2, (**B**) LAP2β and (**C**) emerin (shown in red). Top panels in (A–C) are costained with either anti-dystrophin for the SUN2 and emerin images, or anti-γ-sarcoglycan for the LAP2β images, and shown at 40× magnification to visualize myofibers. Bottom panels in (A–C) are 63× magnification to visualize staining at the nuclear rim. DAPI stains nuclei blue. Scale bar 40× = 10 μm, 63× = 5 μm. (**D**) Immunoblotting of skeletal muscle shows that SUN2 and nesprin-2β are expressed equally in wild-type (+/+) and Δ/ΔKASH mice. Myosin is shown as a loading control (left, bottom panel). (**E**) Coimmunprecipitation from primary myotubes from wild-type and Δ/ΔKASH mice demonstrates that an anti-SUN2 antibody immunoprecipitated wild-type nesprin-1α (*), but not Δ/ΔKASH (right panel). (**F**) Coimmunoprecipitation from COS7 cells cotransfected with Flag-SUN2 and either Xpress-nesprin-1α (WT) or Xpress-Δ/ΔKASH (Δ/Δ) demonstrates that Xpress-Δ/ΔKASH is not immunoprecipitated by Flag-SUN2 (arrow) indicating that Δ/ΔKASH does cannot interact with SUN2.

encoding an additional 61 amino acids derived from intronic genomic sequence. It is notable that in humans there are nesprin-1 isoforms lacking the penultimate exon (15). While we were unable to detect this isoform in wild-type mice (data not shown), it is possible that the penultimate exon is a weak splice acceptor and the absence of the terminal exon causes the penultimate exon to be omitted from the transcript completely.

Of note, a distinct but related model with a disrupted nesprin-1 gene was generated with strikingly different results (23). This model, referred to as syne-$1^{-/-}$, resulted in the absence of nesprin-1 protein from the nuclear membrane and generated no abnormal muscle function. However, this model did show clustering of myonuclei and loss of synaptic nuclei at the neuromuscular junction. Nesprin-1 mutations have been shown to cause Autosomal Recessive Cerebellar

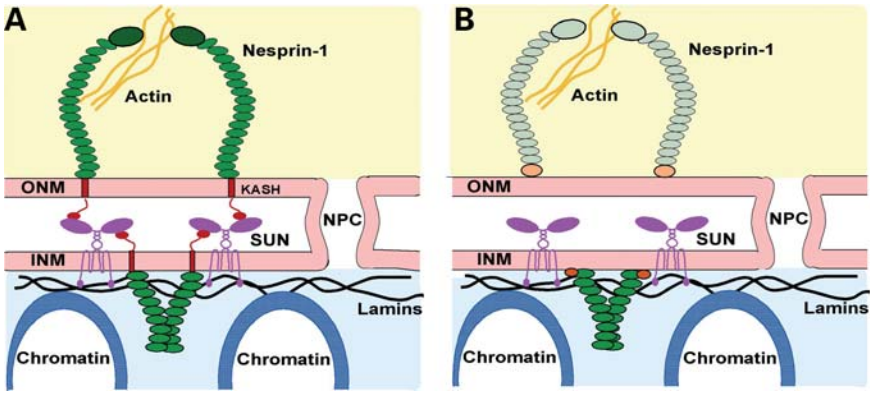

Figure 10. The LINC complex links the nucleoskeleton with the cytoskeleton. (**A**) Nesprin-1 isoforms are tethered to both the inner nuclear membrane and outer nuclear membrane through an N-terminal KASH domain. In the nucleus, nesprin-1 binds lamin A/C filaments that in turn bind other proteins and chromatin. Nesprin-1 interacts with SUN proteins in the lumen of the nuclear envelope. These interactions create a bridge between the nucleus and cytoplasm that may play a role in transmitting signals from the cell surface to the nucleus to affect gene expression. (**B**) The LINC complex in Δ/ΔKASH mice assembles but does not function normally leading to EDMD. ΔKASH protein (shown with orange circle representing alternate C-terminus) cannot interact with the SUN proteins, and therefore the bridge between the cytoplasm and the nucleus is broken leading to neuromuscular disease. The outer nuclear membrane isoforms of nesprin-1 may still be present at the nuclear membrane but do not participate in the LINC complex because no KASH domain is present.

Ataxia (ARCA1) in humans (28). A muscle biopsy from an ARCA1 patient revealed a reduction in the number of synaptic nuclei. Similar to the syne-$1^{-/-}$ mouse model, these patients do not have any overt muscle pathology indicating that loss of synaptic nuclei may have no clinical effect on muscle function. Zhang *et al*., also used a similar strategy to disrupt the related protein nesprin-2 (referred to as syne-$2^{-/-}$). Only in combination did the double mutant, syne-1/syne-2 null, display a phenotype of perinatal lethality. The phenotypic contrast between the syne $1^{-/-}$ model and the Δ/ΔKASH model presented here is likely explained by differences in gene targeting where the Δ/ΔKASH allele is completely missing the terminal coding exon. The mRNA generated from this allele not only lacked the terminal exon but was also missing the penultimate exon and contained an additional 61 novel amino acids. When this mutant protein is assembled into the LINC complex, it is capable of producing defects akin to EDMD. The lack of clinical muscle phenotype in the single syne-$1^{-/-}$ and syne-$2^{-/-}$ models, coupled with the perinatal lethality phenotype in the double null animals, indicates that only one of the two nesprins are required for normal muscle function and that they can substitute for each other in muscle (23). In contrast to the syne-1 null mice that do not express protein, the phenotype in the Δ/ΔKASH mice implicates the formation of a dysfunctional LINC complex because nesprin-1 is expressed with an alternative C-terminal domain (Fig. 10B). We hypothesize that the ΔKASH protein, in its position at the nuclear membrane, occupies binding sites that prevent nesprin-2 from participating in a functional LINC complex and therefore causes muscle disease. An alternative hypothesis is that nesprin-2 is unaffected by the presence of ΔKASH protein and that ΔKASH itself confers a gain of function that disrupts other, possibly unknown, components of the LINC complex. It has been suggested that the disruption of the largest isoforms of nesprin-1 that can localize to the sarcomere contributes to muscle pathology (13). However, electron microscopy on the Δ/ΔKASH skeletal muscle showed normal sarcomere organization (data not shown).

Mice homozygous for the ΔKASH allele exhibit perinatal lethality with approximately half dying at or near birth. Partial perinatal lethality has been described in other mouse models such as the myoglobin null mouse. The majority of embryos lacking myoglobin die from cardiac defects midgestation, while surviving embryos respond to the loss of myoglobin by upregulating genes and increasing myocardial vascularity (29). While the Δ/ΔKASH mice are not as severely affected and live until birth, it is possible that adaptations involving gene expression occur to contribute to survival.

The Δ/ΔKASH mice exhibit phenotypes similar to humans with EDMD and to mice engineered with mutations in the gene encoding lamin A/C. Recent genetic studies in human patients have implicated the nesprins in EDMD. Specifically, DNA variants were identified in the genes encoding nesprin-1 and nesprin-2 in patients with disease ranging from a mild increase in creatine kinase levels to muscular dystrophy with cardiomyopathy (13). Three of the identified variants are missense substitutions in the 3′ end of nesprin-1, where they would be expected to alter both full length nesprin-1 and the shorter nesprin-1α. The nature of these sequence variants and their inheritance pattern with single affected family members makes it difficult to conclude that these variants impart phenotype. A single nesprin-2 missense substitution was also identified that localized to the 5′ end of the nuclear envelope localized isoform, nesprin-2β. The mutations in both nesprin-1 and -2 are located in conserved regions and within the mapped emerin and lamin A/C binding domains (13). Two of the four variants were believed to be sporadic mutations, while the nesprin-2 missense changes were identified in small pedigrees potentially consistent with autosomal dominant inheritance. Fibroblasts from individuals carrying these mutations were shown to have abnormal nuclear morphology much like cultured fibroblasts from EDMD patients with *LMNA* mutations. A minority of cells also exhibited mislocalization of the LINC complex proteins: nesprin, emerin and lamin A/C.

Sex differences have not been noted in human diseases associated with nuclear membrane genes with the exception of those encoded by genes on the X chromosome, such as emerin. Interestingly, we noted a sex difference in Δ/ΔKASH mice where female mice were more uniformly affected from a young age. Female mice surviving to adulthood fail to perform as well as their wild-type littermates in rotarod tests while male mice are statistically indistinguishable from the wild-type counterparts. Among the male mice, affected mice could be seen but the phenotype was more variable. The male phenotype is more apparent at later ages, when we noted kyphoscoliosis, histological and cardiac abnormalities. This suggests that some male mice have protective adaptation in earlier life (before 20 weeks) and that these adaptations fail in later life as both males and females exhibited progressive muscle disease and cardiac defects.

While the data available from patients implicate nesprins in the pathogenesis of neuromuscular disease, our data demonstrate that a normally localized LINC complex is not indicative of normal function and underscores the importance of the LINC complex for cardiac and skeletal muscle disease. The loss of the KASH domain of nesprin-1, along with the generation of the ΔKASH protein, is sufficient to recapitulate many aspects of the EDMD phenotype observed in humans and serve as a model for studying the LINC complex in laminopathy-like disease.

MATERIALS AND METHODS

Generation of the targeting construct

The targeting construct was amplified and cloned from 129 strain mouse DNA. The reference sequence used was MGI:1927152. The 1.9 kb arm was amplified with a forward primer (2kbF 5′-AAGCTTGGAGCTTAGGAAGTTTCTG TTTCACACCCTCTT-3′) and a reverse primer (2kbR2 5′-GCTAGCGCCTGGGTCGCTTCCCTATGACCAAAGGAA CA -3′). This region falls 200 bp upstream of the first codon of the terminal exon. The product was cloned into the *Hin*dIII and *Nhe*I sites of the pPGKneobpAloxX2PGKDTA vector (gift from Dr P. Soriano). The second arm was generated by amplifying a 3.7 kB fragment with a forward primer containing a *Not*I site (4kbF 5′- CCATGGTACAGTTACCAAA CCCAGACACTATTGTGGATT -3′) and a reverse primer containing a *Sac*II site (4kbR3 5′- CCGCGGTACTCCA GTGACAATGTGCTTAGCATGTACGAT -3′). The product was ligated into the *Not*I and *Sac*II sites of pBluescript KS+. A 1.0 kb fragment containing the terminal exon and 200 bp of upstream and downstream flanking sequence was amplified with a forward primer containing a *Not*I site (Ex17F 5′-GCGGCCGCCAGCCTACAGAAGGCTCACAGA TCTTATCTC -3′) and a reverse primer with a *Nco*I site (Ex17R2 5′- CCATGGATATGGGATGAATGCCCAGGTGG GACAGTCTTT -3′). The product was ligated into TOPO pCR 2.1 and then into the *Not*I and *Sac*I sites of pBluescript KS+ to create Ex17pBluescript. To create the loxP site flanking the 3′ end of the terminal exon, forward and reverse primers with *Nco*I sites at the 5′ and 3′ ends (LoxPF3 5′- CATGGATA ACTTCGTATAATGTATGCTATACGAAGTTAT; LoxPR3 5′-CTATTGAAGCATATTACATACGATATGCTTCAATA AGTAC -3′) were annealed together and cloned into the *Nco*I site of Ex17pBluescript. Ex17pBluescript was ligated to pBluescript KS+ at the *Not*I and *Nco*I sites. This construct was then subcloned into the pPGKneobpAloxX2PGKDTA vector containing the short arm, using the *Not*I and *Sac*II sites.

Homologous recombination in embryonic stem cells

The targeting vector was linearized with *Sac*II and electroporated into 2.0×10^7 PRX-129/S6 embryonic stem cells (Primogenix) with a Gene Pulser (Bio-Rad) at 250 V in a 0.4 cm electrode gap cuvette. Cells were plated on inactivated mouse embryonic fibroblasts (Specialty Media) and after 24 h were selected with 250 μg/ml G418 (Invitrogen). Five clones out of 235 screened contained the recombined allele as determined by Southern blotting. Clones were digested with *Eco*RI, separated on a 0.8% GTG agarose gel (Seakem) and blotted on Hybond-*N*+nylon membrane (Amersham Biosciences). The probe for blotting was amplified using Nesp5F 5′- AATAAT GAAAGGAATACCAGAGAAGCA -3′) and Nesp6R (5′-AACAGTAGTCAAATGACACATTAAAAA -3′). The wild-type allele yields a 6.1 kB fragment while the recombined allele yields a 4.9 kb fragment.

Generation of chimeric animals

Two independent ES cell clones were injected into C57BL blastocysts and implanted into pseudopregnant females. Animals born from ES cell-injected blastocysts displayed chimerism in coat color, ranging from 70 to 90%. Chimeric males were bred to C57BL mice producing mice on a mixed C57BL/129 background. Female mice heterozygous for the targeted allele were bred to male mice expressing cre recombinase in the germline (129-Tg(Prm-cre)58Og/J, Jackson Laboratory). Using PCR primers 1, 2 and 3 (Primer 1 5′- CATCCTTTCG-CAGAACTGTTCCTTTGG -3′, Primer 2 5′- CATTTCC-CAACCACCGAGATAAG -3′, Primer 3 5′- GAGCATCCA CCTTTGTAAGGCTCTGG -3′) genotyping of mouse tail DNA confirmed recombination of loxP sites resulting in loss of the neomycin cassette and the terminal exon. Heterozygote mice were intercrossed to maintain the line.

Isolation of RNA and 3′RACE

Total RNA was extracted from littermate and homozygous Δ/ΔKASH mouse skeletal muscle using a standard Trizol RNA isolation protocol (Invitrogen). 3′RACE (rapid amplification of cDNA ends) was performed using the First Choice RLM-RACE kit (Ambion) according to the manufacturer's protocol. In 3′RACE the first-strand cDNA is synthesized from total RNA using the 3′-RACE adaptor included in the kit. cDNA was then subjected to nested PCR using the 3′-RACE primers provided in the kit that are complementary to the 3′-adaptor and two upstream gene-specific primers (MmRTPCRF1 5′-GCCTCACTACAAGACATGTCTCGCC AACTC -3′; MmRTPCRF2 5′-AAGGAGGTCAGCCATC ATATCAAGGATCTT-3′). Cycling conditions for both outer and inner 3′-RLM-RACE PCR were: 94°C for 2 min, followed by 30 cycles, 94°C for 30 s, 58°C for 1 min, 72°C for 1 min,

with a final extension of 10 min. PCR products were cleaned in an S-300 column (Amersham Biosciences) and sequenced.

Generation of primary myoblasts

P0 offspring from heterozygous crosses were sacrificed. Hind and fore legs including shoulder and back were harvested and the skin removed. Muscle and bone were minced in 500 μl PBS in a sterile Petri dish. The particulate matter was removed. Blendzyme 3 (Roche) was added to the pellet at a concentration of 0.22 mg per 0.3 g of muscle. Muscle was incubated at 37°C and triturated every 10 min after 1 h, the slurry was filtered through a 100-μm filter and centrifuged for 5 min. Cells were resuspended in primary media (F-10 HAM's with 20% FBS, 1%PSA and 2.5 ng/ml bFGF) (Invitrogen, Fisher). Cells were preplated on gelatinized 60 mm dishes at 37°C for 20 min, then transferred to 60 mm gelatinized plates for growth. Myoblasts were grown to confluence and differentiated in differentiation media (DMEM with 2% horse serum and 1%PSA) (Invitrogen).

Generation of Nesprin-2 antibody

The peptide, ETESRVPGSTRPQRS, representing residues 1542–1587 of GenBank accession no. AY061758 was synthesized and injected into rabbits to raise a polyclonal antisera (Zymed Laboratories, South San Francisco, CA). A glutathione s-transferase (GST) fusion protein expressing a fragment of nesprin-2 (amino acids 337–502) was expressed in *E.coli* using pGEX4T-3 (GE Healthcare) and was used to affinity purify nesprin-2 as described (30).

Immunoblotting and immunofluorescence microscopy

Differentiated primary myoblasts from Δ/ΔKASH mice and wild-type littermates were lysed on ice in cell lysis buffer (10 mM Tris pH 7.0, 1 mM EDTA pH 8.0, 150 mM NaCl, 1% TritonX100) with protease inhibitors (Complete protease inhibitor mixture, Roche Molecular Biochemicals). Cellular debris was removed by centrifugation at 16 000*g* for 15 min at 4°C and the protein concentration of the supernatant was assayed with a Bio-Rad protein assay. Twenty-five micrograms of protein was separated by SDS–PAGE followed by either GelCode blue stain reagent (Pierce) or electrophoretic transfer to polyvinylidene difluoride Immobilon-P membrane (Millipore). The membrane was blotted with nesprin-1 antibodies, AN1 antibody (15) at 1:300 or MANNES1A (http://www.newi.ac.uk/research/mric/mono/monoabs.htm) at 1:50 or Nesprin-2 at 1:500 in 1%BSA in 1×Tris-buffered saline plus 0.1% Tween. Secondary antibody conjugated to horseradish peroxidase (Jackson Immunochemicals) was used at 1:5000. ECL-Plus (Amersham Biosciences) was used for detection of the secondary and visualized on Kodak Biomax MS film.

Quadriceps muscles from 10- to 12-week-old and 9- to 12-month old Δ/ΔKASH mice and wild-type littermates were harvested and frozen in liquid nitrogen-cooled isopentane. Frozen 7 μm sections were fixed in ice-cold methanol for 2 min, rinsed in PBS and blocked with 5% FBS in PBS with 0.1%Triton for 1 h at room temperature. Primary antibodies used and their concentrations were: AN1 1:100; anti-Lamin A/C (SC 20681 Santa Cruz) 1:30; anti-SUN2 (31) 1:1000; anti-emerin (Novocastra) 1:250; and anti-LAP2β (cat. no. 611000, BD Biosciences) 1:250. Sarcolemmal markers used to outline myofibers were anti-γ-sarcoglycan (30) at 1:250 or anti-dystropin (Novocastra, NCL-DYS3) at 1:100. Sections were incubated with primary antibody in blocking buffer at 4°C overnight. Secondary antibodies conjugated to either Cy3 or Alexa 488 were incubated at room-temperature for 1 h, sections were mounted in Vectashield with 4′,6-diamidimo-2-phenylindole (DAPI) (Vector Labs) and images were captured with an Axiophot microscope and Axiovision (Carl Zeiss) software.

Recombinant constructs

Full length nesprin-1α was PCR amplified from MGC clone ID 6492523 (Invitrogen) with a forward primer (*Kpn*IF 5′-GATCGGTACCTATGGTGGTGGCAGAGGACTTGCAT-3′) and a reverse primer (*Not*IR 5′-CATGGCGGCCGCTCAGAG TGGAGGAGGACCGT-3′) and ligated in frame with the Xpress tag of pcDNA3.1 HisB (Invitrogen). The 3′ end of Δ/ΔKASH was amplified from cDNA generated from Δ/ΔKASH skeletal muscle and cloned into TOPOpCR2.1 (Invitrogen). The 3′ fragment was subcloned in pBluescript KS+ (Stratagene), and an XbaI site common to both wild-type and Δ/ΔKASH was used to further subclone the Δ/ΔKASH 3′ end into pcDNA3.1 HisB containing the 5′ end of nesprin-1α. Full length SUN2 was PCR amplified from Fantom clone ID F630221N03 (DNAFORM) with a forward primer (SUN2F 5′-GATCGGAATTCTATGTCGAGACGAAGCCAGCG-3′) and a reverse primer (SUN2R 5′-GCGGCCGCGACTGGG CAGGCTCTCDCGTG-3′) and cloned in frame with a FLAG tag inserted into pcDNA3 (Invitrogen).

Immunoprecipitation of SUN2 and Nesprin-1 from primary myoblasts

For immunoprecipitations, primary myoblasts from wild-type and Δ/ΔKASH mice were harvested and processed as described (25). Briefly, lysates were sonicated in immunoprecipitation buffer (10 mM HEPES, pH7.4, 10 mM KCl, 5 mM EDTA, 1% Triton-100 and protease inhibitor cocktail) and then centrifuged at 16 000*g* for 15 min at 4°C. Lysate was then precleared with protein A/G sepharose. Immunoprecipitations with SUN2 or AN1 (dilutions 1:75) were performed at room temperature for 3 h with agitation, followed by incubation for 2 h with Protein A/G sepharose and centrifugation for 10 min at 4000*g*. Beads were washed four times and proteins were eluted with SDS sample buffer and run on 10% SDS–PAGE. Proteins were transferred to PVDF membrane and blocked for 1 h in 1% BSA/TBS-T and incubated overnight in SUN2, 1:500. The membrane was stripped in 2% SDS, 60 mM Tris, pH6.8, and 0.1% 2-mercaptoethanol for 30 min at 50°C. The membrane was then blotted with AN1, 1:300 overnight. Secondary antibodies were applied as earlier.

Immunoprecipitation of SUN2 and Nesprin-1 from transfected COS7 cells

COS7 cells maintained in Dulbecco's modified Eagle's medium with 10% fetal bovine serum were grown to 80% confluence and transfected with FLAG-SUN2 and either Xpress-nesprin-1α or Xpress-Δ/ΔKASH using the *Trans*-It LT1 transfection reagent per manufacturer's instructions (Mirus Bio). Twenty-four to forty-eight hours post-transfection, lysates were prepared and immunoprecipitation was performed as earlier using the αFLAG polyclonal antibody (Sigma).

Perinatal lethality analysis

Heterozygous intercrosses of +/ΔKASH animals were performed and mice were genotyped at P21. To determine time of death of Δ/ΔKASH mice, pregnant females from the heterozygous intercrosses, where sacrificed between E17.5 and P0 and embryos were removed and genotyped. Pregnant females from heterozygous intercrosses were observed giving birth and pups were monitored. After expiration of any pups from these births, the lungs were dissected and examined.

Rotarod experiments

Six mice from each genotype, three males and three females, were selected to participate in the rotarod studies. Between 8 and 16 weeks of age, mice were run once a week at the same time each week. All mice were placed on the rod in identical positions to start each run. Each test consisted of three runs ending when the mouse fell off the rod, gripped the rod and revolved or reached 5 min whichever came first. Total time for each run was recorded. Angles were scored by marking the rotarod at 15° intervals and determining the angle of the shoulder in relation to the rod. The angle was scored as 0 when the mouse shoulder was parallel to the top of the rod. Higher angles were scored as the mouse shoulders moved back on the rod. Angles were scored every 30 s for the duration of each run. To analyze the data, the average angle over all three runs was calculated for each mouse and a *t*-test was performed.

Histology

Seven mice, three wild-type and three Δ/ΔKASH, both males and females, 9–13 months old, were sacrificed and the skeletal muscle was harvested. Muscle was preserved in 10% formalin, bisected at the mid-belly and imbedded in paraffin. Sections were stained with hematoxylin & eosin. The entire cross-section of the mid-soleus was counted for fiber number and central nuclei. Fiber size was determined using ImageJ, each fiber per soleus was measured. Prism software was used to analyze the results.

Visualizing nuclei in muscle fibers

Tibialis anterior and triceps muscle from wild-type and Δ/ΔKASH mice were harvested and fixed in 4% paraformaldehyde for 20 min. Fibers were teased apart and individual fibers were mounted in Vectashield with DAPI (Vector Laboratories). An Olympus DSU microscope was used to image the nuclei.

Ambulatory ECG recordings

Continuous ambulatory ECG recordings were obtained as previously described (32). Nine to 12-month-old mice were used for analysis. Recording was performed for 24–30 h. Data were analyzed using Physiostat ECG analysis 4.0 software (Transoma Medical, St Paul, MN). Each waveform was measured for heart rate, PR, QRS and QT intervals, values were compiled for wild-type and Δ/Δ animals and compared using a *t*-test.

Conflict of Interest statement. None declared.

FUNDING

Supported by the Muscular Dystrophy Association, the American Heart Association (to M.J.P.) and NIH HL092443 (to E.M.M.).

REFERENCES

1. Favreau, C., Dubosclard, E., Ostlund, C., Vigouroux, C., Capeau, J., Wehnert, M., Higuet, D., Worman, H.J., Courvalin, J.C. and Buendia, B. (2003) Expression of lamin A mutated in the carboxyl-terminal tail generates an aberrant nuclear phenotype similar to that observed in cells from patients with Dunnigan-type partial lipodystrophy and Emery-Dreifuss muscular dystrophy. *Exp. Cell Res.*, **282**, 14–23.
2. Bonne, G., Mercuri, E., Muchir, A., Urtizberea, A., Becane, H.M., Recan, D., Merlini, L., Wehnert, M., Boor, R., Reuner, U. *et al.* (2000) Clinical and molecular genetic spectrum of autosomal dominant Emery-Dreifuss muscular dystrophy due to mutations of the lamin A/C gene. *Ann. Neurol.*, **48**, 170–180.
3. Wang, Y., Herron, A.J. and Worman, H.J. (2006) Pathology and nuclear abnormalities in hearts of transgenic mice expressing M371K lamin A encoded by an LMNA mutation causing Emery-Dreifuss muscular dystrophy. *Hum. Mol. Genet.*, **15**, 2479–2489.
4. Sullivan, T., Escalante-Alcalde, D., Bhatt, H., Anver, M., Bhat, N., Nagashima, K., Stewart, C.L. and Burke, B. (1999) Loss of A-type lamin expression compromises nuclear envelope integrity leading to muscular dystrophy. *J. Cell Biol.*, **147**, 913–920.
5. Arimura, T., Helbling-Leclerc, A., Massart, C., Varnous, S., Niel, F., Lacene, E., Fromes, Y., Toussaint, M., Mura, A.M., Keller, D.I. *et al.* (2005) Mouse model carrying H222P-Lmna mutation develops muscular dystrophy and dilated cardiomyopathy similar to human striated muscle laminopathies. *Hum. Mol. Genet.*, **14**, 155–169.
6. Maioli, M.A., Marrosu, G., Mateddu, A., Solla, E., Carboni, N., Tacconi, P., Lai, C. and Marrosu, M.G. (2007) A novel mutation in the central rod domain of lamin A/C producing a phenotype resembling the Emery-Dreifuss muscular dystrophy phenotype. *Muscle Nerve*, **36**, 828–832.
7. Sewry, C.A., Brown, S.C., Mercuri, E., Bonne, G., Feng, L., Camici, G., Morris, G.E. and Muntoni, F. (2001) Skeletal muscle pathology in autosomal dominant Emery-Dreifuss muscular dystrophy with lamin A/C mutations. *Neuropathol. Appl. Neurobiol.*, **27**, 281–290.
8. Charniot, J.C., Pascal, C., Bouchier, C., Sebillon, P., Salama, J., Duboscq-Bidot, L., Peuchmaurd, M., Desnos, M., Artigou, J.Y. and Komajda, M. (2003) Functional consequences of an LMNA mutation associated with a new cardiac and non-cardiac phenotype. *Hum. Mutat.*, **21**, 473–481.
9. Mounkes, L.C., Kozlov, S.V., Rottman, J.N. and Stewart, C.L. (2005) Expression of an LMNA-N195K variant of A-type lamins results in cardiac conduction defects and death in mice. *Hum. Mol. Genet.*, **14**, 2167–2180.

10. Bonne, G., Di Barletta, M.R., Varnous, S., Becane, H.M., Hammouda, E.H., Merlini, L., Muntoni, F., Greenberg, C.R., Gary, F., Urtizberea, J.A. *et al.* (1999) Mutations in the gene encoding lamin A/C cause autosomal dominant Emery-Dreifuss muscular dystrophy. *Nat. Genet.*, **21**, 285–288.
11. Mounkes, L.C., Kozlov, S., Hernandez, L., Sullivan, T. and Stewart, C.L. (2003) A progeroid syndrome in mice is caused by defects in A-type lamins. *Nature*, **423**, 298–301.
12. Bonne, G., Yaou, R.B., Beroud, C., Boriani, G., Brown, S., de Visser, M., Duboc, D., Ellis, J., Hausmanowa-Petrusewicz, I., Lattanzi, G. *et al.* (2003) 108th ENMC International Workshop, 3rd Workshop of the MYO-CLUSTER project: EUROMEN, 7th International Emery-Dreifuss Muscular Dystrophy (EDMD) Workshop, 13–15 September 2002, Naarden, The Netherlands. *Neuromuscul. Disord.*, **13**, 508–515.
13. Zhang, Q., Bethmann, C., Worth, N.F., Davies, J.D., Wasner, C., Feuer, A., Ragnauth, C.D., Yi, Q., Mellad, J.A., Warren, D.T. *et al.* (2007) Nesprin-1 and -2 are involved in the pathogenesis of Emery Dreifuss muscular dystrophy and are critical for nuclear envelope integrity. *Hum. Mol. Genet.*, **16**, 2816–2833.
14. Zhang, Q., Skepper, J.N., Yang, F., Davies, J.D., Hegyi, L., Roberts, R.G., Weissberg, P.L., Ellis, J.A. and Shanahan, C.M. (2001) Nesprins: a novel family of spectrin-repeat-containing proteins that localize to the nuclear membrane in multiple tissues. *J. Cell. Sci.*, **114**, 4485–4498.
15. Mislow, J.M., Kim, M.S., Davis, D.B. and McNally, E.M. (2002) Myne-1, a spectrin repeat transmembrane protein of the myocyte inner nuclear membrane, interacts with lamin A/C. *J. Cell. Sci.*, **115**, 61–70.
16. Zhen, Y.Y., Libotte, T., Munck, M., Noegel, A.A. and Korenbaum, E. (2002) NUANCE, a giant protein connecting the nucleus and actin cytoskeleton. *J. Cell. Sci*, **115**, 3207–3222.
17. Apel, E.D., Lewis, R.M., Grady, R.M. and Sanes, J.R. (2000) Syne-1, a dystrophin- and Klarsicht-related protein associated with synaptic nuclei at the neuromuscular junction. *J. Biol. Chem.*, **275**, 31986–31995.
18. Warren, D.T., Zhang, Q., Weissberg, P.L. and Shanahan, C.M. (2005) Nesprins: intracellular scaffolds that maintain cell architecture and coordinate cell function? *Expert Rev. Mol. Med.*, **7**, 1–15.
19. Padmakumar, V.C., Libotte, T., Lu, W., Zaim, H., Abraham, S., Noegel, A.A., Gotzmann, J., Foisner, R. and Karakesisoglou, I. (2005) The inner nuclear membrane protein Sun1 mediates the anchorage of Nesprin-2 to the nuclear envelope. *J. Cell. Sci.*, **118**, 3419–3430.
20. Haque, F., Lloyd, D.J., Smallwood, D.T., Dent, C.L., Shanahan, C.M., Fry, A.M., Trembath, R.C. and Shackleton, S. (2006) SUN1 interacts with nuclear lamin A and cytoplasmic nesprins to provide a physical connection between the nuclear lamina and the cytoskeleton. *Mol. Cell. Biol.*, **26**, 3738–3751.
21. Crisp, M., Liu, Q., Roux, K., Rattner, J.B., Shanahan, C., Burke, B., Stahl, P.D. and Hodzic, D. (2006) Coupling of the nucleus and cytoplasm: role of the LINC complex. *J. Cell. Biol.*, **172**, 41–53.
22. O'Gorman, S., Dagenais, N.A., Qian, M. and Marchuk, Y. (1997) Protamine-Cre recombinase transgenes efficiently recombine target sequences in the male germ line of mice, but not in embryonic stem cells. *Proc. Natl Acad. Sci. USA*, **94**, 14602–14607.
23. Zhang, X., Xu, R., Zhu, B., Yang, X., Ding, X., Duan, S., Xu, T., Zhuang, Y. and Han, M. (2007) Syne-1 and Syne-2 play crucial roles in myonuclear anchorage and motor neuron innervation. *Development*, **134**, 901–908.
24. Pare, G.C., Easlick, J.L., Mislow, J.M., McNally, E.M. and Kapiloff, M.S. (2005) Nesprin-1alpha contributes to the targeting of mAKAP to the cardiac myocyte nuclear envelope. *Exp. Cell Res.*, **303**, 388–399.
25. Mislow, J.M., Holaska, J.M., Kim, M.S., Lee, K.K., Segura-Totten, M., Wilson, K.L. and McNally, E.M. (2002) Nesprin-1alpha self-associates and binds directly to emerin and lamin A *in vitro*. *FEBS Lett.*, **525**, 135–140.
26. Muchir, A., Van Engelen, B., Lammens, M., Mislow, J.M., McNally, E.M., Schwartz, K. and Bonne, G. (2003) Nuclear envelope alterations in fibroblasts from LGMD1B patients carrying nonsense Y259X heterozygous or homozygous mutation in lamin A/C gene. *Exp. Cell Res.*, **291**, 352–362.
27. Stewart-Hutchinson, P.J., Hale, C.M., Wirtz, D. and Hodzic, D. (2008) Structural requirements for the assembly of LINC complexes and their function in cellular mechanical stiffness. *Exp. Cell Res.*, **314**, 1892–1905.
28. Gros-Louis, F., Dupre, N., Dion, P., Fox, M.A., Laurent, S., Verreault, S., Sanes, J.R., Bouchard, J.P. and Rouleau, G.A. (2007) Mutations in SYNE1 lead to a newly discovered form of autosomal recessive cerebellar ataxia. *Nat. Genet.*, **39**, 80–85.
29. Meeson, A.P., Radford, N., Shelton, J.M., Mammen, P.P., DiMaio, J.M., Hutcheson, K., Kong, Y., Elterman, J., Williams, R.S. and Garry, D.J. (2001) Adaptive mechanisms that preserve cardiac function in mice without myoglobin. *Circ. Res.*, **88**, 713–720.
30. McNally, E.M., Duggan, D., Gorospe, J.R., Bonnemann, C.G., Fanin, M., Pegoraro, E., Lidov, H.G., Noguchi, S., Ozawa, E., Finkel, R.S. *et al.* (1996) Mutations that disrupt the carboxyl-terminus of gamma-sarcoglycan cause muscular dystrophy. *Hum. Mol. Genet.*, **5**, 1841–1847.
31. Hodzic, D.M., Yeater, D.B., Bengtsson, L., Otto, H. and Stahl, P.D. (2004) Sun2 is a novel mammalian inner nuclear membrane protein. *J. Biol. Chem.*, **279**, 25805–25812.
32. Chutkow, W.A., Pu, J., Wheeler, M.T., Wada, T., Makielski, J.C., Burant, C.F. and McNally, E.M. (2002) Episodic coronary artery vasospasm and hypertension develop in the absence of Sur2 K(ATP) channels. *J. Clin. Invest.*, **110**, 203–208.